Viscoplastic Response of Unidirectional Fiber Polymer Composites

E.KONTOU AND A.KALLIMANIS

School of Applied Mathematical and Physical Sciences
Department of Mechanics
National Technical University of Athens, 5 Heroes of Polytechnion, GR-15773, Athens, Greece

ABSTRACT: Unidirectional glass fiber composites materials based on an epoxy matrix were studied in terms of tensile experiments at various strain rates. The theoretical procedure for the prediction of the tensile behavior of the off-axis specimens was based on a flow rule for orthotropic material, the kinematics of the multiplicative decomposition , as well as a micromechanical model to expressing the rate of plastic deformation. A satisfactory agreement between experimental data and calculated results was found , while the rate effect was predicted in terms of a scaling rule.

Key words: material anisotropy, viscoplasticity, fiber composites, nonlinearity, rate effect.

1. INTRODUCTION

The departure from linearity in several types of loading is one of the main features of unidirectional fiber composites, made of fibers and thermoplastic or thermosetting resins [1,2] . A lot of theories were developed to formulate this non linear stress-strain relationship [1,3,5]. An extensive study was made [5] for boron/aluminum and graphite/epoxy fiber composites. A one parameter flow rule for orthotropic plasticity was developed, and a plastic potential with this single parameter gave accurate calculations. Moreover, this one parameter plastic potential function was the basis for the introduction of two rate dependent models to describe the material behavior.

Another essential feature of unidirectional polymer-fiber composites is the strain-rate response that they exhibit, making of primary interest the prediction of the mechanical behavior of these materials to dimension structural elements.

Several approaches have also been made regarding the strain-rate response of fiber reinforced composites. An elastic–viscoplastic constitutive model has been developed [6], leading to the evaluation of a quasi-static stress-strain curve. An effective stress/effective plastic strain curve was established [5] in terms of a power law, containing two more parameters.

Recently, this strain rate response has been treated as a viscoelastic behavior induced by the properties of the matrix [7]. These approaches include a phenomenological macroscopic analysis or a micromechanics study, which calculate the behavior of the composite through the characteristics of the components.

In the present work, in order to describe the nonlinear behavior of polymer matrix-fiber composites, a theoretical model is proposed, which is based on some basic assumptions: The tensile behavior of the composite materials is considered to be a plane -stress, plane- strain problem. The multiplicative decomposition of the deformation gradient F into the elastic and plastic part, developed by Lee et al [8] is also considered to be valid. Moreover, an associated flow rule for an orthotropic material based on a dyadic of vectors $\mathbf{a_i}$ parallel to the material axes is introduced for our analysis. The functional form of the rate of plastic deformation, which was analytically presented in previous works [9,10], has also been applied in our theoretical approach.

On the other hand, tensile experiments were performed on off-axis epoxy-glass fiber composites at various strain rates. The theoretical results were found to be adequately close to the experimental ones.

2. KINEMATICS OF FINITE PLASTIC DEFORMATION

Our analysis is based on the multiplicative decomposition of the deformation gradient F proposed by Lee at al [8], and on the additive decomposition of the deformation rate. During the deformation of a work-hardening material, both elastic and plastic deformations are generated to give the total deformation. When the load is removed, the material is assumed to return to a zero stress-state, while the elastic strain is recovered. The remaining strain at the zero stress-state is termed the plastic strain. According to those statements, the following well known multiplicative decomposition of the deformation gradient is obtained:

$$F = F^e F^p \tag{1}$$

where F is the deformation gradient tensor, F^p is the plastic deformation gradient, resulting from the original configuration to an intermediate configuration of pure plastic deformation, and F^e the elastic deformation gradient, relating the intermediate configuration with the current one, in terms of elastic deformation.

From the definition for the Lagrangian strain tensor E:

$$E = \frac{1}{2}\left(F^T F - I\right) \tag{2}$$

where I is the identity tensor,

it follows that the elastic strain tensor E^e is given by:

$$E^e = \frac{1}{2}\left[\left(F^e\right)^T F^e - I\right] \tag{3}$$

where E^e is the strain tensor measured relative to the intermediate configuration, for the deformation from the unstressed configuration to the current configuration and hence it represents pure elastic strain [11].

On the other hand, for the velocity gradient tensor L the following equations hold:

$$L = D + W, \qquad L^e = D^e + W^e, \qquad L^p = D^p + W^p \tag{4}$$

where D, D^e,D^p and W,W^e,W^p are respectively the symmetric and antisymmetric parts of L, L^e and L^p.
The terms D^p and W^p must be both constitutively described. Due to the small strains exhibited by the materials tested, the plastic spin W^p is considered to be negligible.
A set of orthonormal vectors $\mathbf{a_i}$ that follow the material axes, forming an angle θ with the direction x of tension was taken into account,as it is shown in Fig.1:
The vectors are defined as follows:

$$\mathbf{a_1} = (\cos\theta, \sin\theta), \quad \mathbf{a_2} = (-\sin\theta, \cos\theta)$$

(5)

The directions of the symmetric part of the plastic velocity gradient tensor D^p will consequently be defined in respect to the dyadic $\mathbf{a_1} \otimes \mathbf{a_2}$ [12,13].
Therefore, the flow rule that determines the rate of plastic deformation is given by the expression:

$$D^p = \dot{F}_p \, \tilde{D}^p$$

(6)

where $\dot{F}_p$ is a non-negative function that was introduced in previous works [9.10] and will be presented in detail in the following.
The quantity $\tilde{D}^p$ defines the directions of D^p , based on the dyadic $\mathbf{a_1} \otimes \mathbf{a_2}$ as already mentioned, through the expression:

$$\begin{aligned}\tilde{\mathbf{D}}^p &= b_{11}[\mathbf{T}' \bullet (\mathbf{a_1} \otimes \mathbf{a_1})](\mathbf{a_1} \otimes \mathbf{a_1} - 0.5a_{11}\mathbf{I})/\tau + \\ & b_{22}[\mathbf{T}' \bullet (\mathbf{a_2} \otimes \mathbf{a_2})](\mathbf{a_2} \otimes \mathbf{a_2} - 0.5a_{22}\mathbf{I})/\tau + \\ & b_{12}[\mathbf{T}' \bullet (\mathbf{a_1} \otimes \mathbf{a_2})](\mathbf{a_1} \otimes \mathbf{a_2})/\tau\end{aligned}$$

(7)
where b_{ij} is a set of non-negative constants expressing the amount of contribution to the plastic strain rate in the various directions [12] , denoting this way the anisotropic character of the material. $\mathbf{T}'$ is the deviatoric stress tensor, and every term of Eq. (6) is normalized by division with the maximum shear stress τ, assuming that yield takes place mainly in the direction of τ.

The quantity $\dot{F}_p$ which expresses the rate of plastic deformation, has been analytically presented in previous works [13,14] and its form has been derived following the assumption that strain is accumulated around specific regions into the material. When the corresponding strain energy around each region reaches a critical value, a non-reversible transition takes place, relative to the emergence of plastic deformation.
Making the further assumption that the strain around each region follows a normal distribution with a mean value m and a standard deviation s, and at the onset of yielding, $\dot{F}_p$ becomes equal to the effective strain rate imposed, it was finally obtained that $\dot{F}_p$ is given by the expression:

$$\dot{F}_{p} = \frac{\dot{\varepsilon}}{s\sqrt{2\pi}} \int_{0}^{\varepsilon} \exp\left[-\frac{1}{2}\left(\frac{\varepsilon_{i} - m}{s} \right)^{2} \right] d\varepsilon_{i} \tag{8}$$

where $\dot{\varepsilon}$ is the imposed effective strain rate and ε is the strain .

For the description of the strain-rate effect, the concept of the scaling rules of viscoelasticity [14] will be expanded here. Following these rules, a stress-strain curve at a strain rate $\dot{\varepsilon}_2$ can be obtained from a corresponding curve at a rate $\dot{\varepsilon}_1$ by multiplying the stress and strain with the scaling factors $\left(\frac{\dot{\varepsilon}_2}{\dot{\varepsilon}_1}\right)^{a}$ and $\left(\frac{\dot{\varepsilon}_2}{\dot{\varepsilon}_1}\right)^{b}$ correspondingly. This concept was used in our case for the scaling of parameter m of the distribution function of Eq.(8), according to the expression:

$$m \rightarrow m\left(\frac{\dot{\varepsilon}_2}{\dot{\varepsilon}_1}\right)^{n} \tag{9}$$

3. CONSTITUTIVE EQUATIONS

The constitutive equations for an orthotropic material expressed in respect to the material axes in a two dimensional problem are given by:

$$\begin{bmatrix} T_{11} \\ T_{22} \\ T_{12} \end{bmatrix} = \begin{bmatrix} Q_{11} & Q_{12} & 0 \\ Q_{12} & Q_{22} & 0 \\ 0 & 0 & 2Q_{66} \end{bmatrix} \begin{bmatrix} e_{11} \\ e_{22} \\ e_{12} \end{bmatrix} \tag{10}$$

where the matrix coefficients Q_{ij} can be written in terms of the engineering constants as:

$$Q_{11} = \frac{E_1}{1 - \nu_{12}\nu_{21}}$$

$$Q_{12} = \frac{\nu_{12}E_2}{1 - \nu_{12}\nu_{21}} = \frac{\nu_{21}E_1}{1 - \nu_{12}\nu_{21}}$$

$$Q_{22} = \frac{E_2}{1 - \nu_{12}\nu_{21}}$$

$$Q_{66} = G_{12}$$

(11)

The constitutive Eq.(10) can be transformed to the x-y coordinate system, taking the form:

$$\begin{bmatrix} T_{xx} \\ T_{yy} \\ T_{xy} \end{bmatrix} = \begin{bmatrix} \overline{Q}_{11} & \overline{Q}_{12} & 0 \\ \overline{Q}_{12} & \overline{Q}_{22} & 0 \\ 0 & 0 & 2\overline{Q}_{66} \end{bmatrix} \begin{bmatrix} e_{xx} \\ e_{yy} \\ e_{xy} \end{bmatrix}$$

(12)

where $\overline{Q}_{ij}$ are the transformed reduced stiffnesses or off-axis reduced stiffnesses .

4. MATERIALS-EXPERIMENTS

Unidirectional glass-fiber composites with an epoxy-vinyl resin (under the commercial name *DERAKANE 411-45*) as a matrix were examined. The physical properties of the epoxy resin used are: viscosity = 440 cP, Density= 1.04 g/cm^3, gel time = 10-60 min.

Off -axis coupon specimens were cut at angles of 0^0, 15^0, 30^0 and 45^0. Fiber –glass end tabs 25 mm in length were adapted to the specimens at each end using an epoxy glue, resulting in specimens with 100mm gage length and 18 mm width The tensile experiments were performed at room temperature with an Instron 1121 type tester at three different strain rates, namely 8.33 10^{-5}, 3.33 10^{-4}, 1.66 10^{-3} sec^{-1}. The deformation could be measured very accurately at every localized region, along the total gauge length. The experimental procedure followed, is based on a non-contact method with a laserextensometer, described in detail elsewhere [15]. True stress – strain curves were then constructed in respect to that part of the gauge length that exhibits the maximum deformation.

Stress-strain results of unidirectional specimens are shown in Fig.2. From this figure is shown that the material exhibits neither plasticity nor strain-rate effect in the fiber direction. The stress-strain curves at the above mentioned strain rates for off-axis specimens of 15^0, 30^0 and 45^0 are presented in Fig. 3,4,5. The strain rate effect is obvious for all types of coupon specimens.

5. MODELING THE TENSILE EXPERIMENTS OF THE OFF-AXIS SPECIMENS

Taking into account the above presented kinematic formulation, the flow rule for an orthotropic material in a two-dimensional problem, and the constitutive equations, we have made numerical calculations using the software *Mathematica*® [16], according to the following procedure:

Working with reference the material axes 1-2, and combining eq. (1) and (2), as well as the flow rule of eq. (7), the time derivatives of plastic strains could be obtained. The integration was made numerically, using small time steps, until high convergence could be obtained. Hereafter, the two components of the elastic strain tensor were obtained. Through the constitutive eq.(10) the stress components were evaluated. The stresses were then transformed in terms of angle θ to evaluate the stresses with reference to the x-y axes. The additional condition that both T_{xy}, T_{yy} are equal to zero, results to the calculation of the unknown component of strain. Finally, the stress T_{xx} versus strain ε_{xx} was obtained.

According to the presented analysis, the unknown parameters are the b_{ij} constants, the mean value m, and the power coefficient n of eq. (9).

The coefficient b_{11} was taken equal to zero, denoting this way that there is no plasticity in the direction parallel to the fibers. Constants b_{22} and b_{12} were fitted to be equal to 0.6 and 2.0 respectively.

The elastic constants of the fiber-epoxy composites were as follows:

E_1=23 GPa, E_2=5.43 GPa, ν_{12}=0.254 and G_{12}=4.7 GPa.

To predict the tensile experimental results at the various strain rates, the scaling rule of eq. (9) was applied. It was found that for the better approximation of the experimental results at the various values of the angle θ, parameter m should change slightly for the off-axis specimens of angle 15^0, 30^0 and 45^0 taking the average value of 0.003. As it has been abovementioned, this parameter m expresses the value of strain at which nonlinearity (onset of yielding takes place). The standard deviation s was taken equal to m/2. The power coefficient n was fitted to be equal to 0.1, in our experimental results.

The theoretical results for the three strain rates examined are presented in comparison with the experimental data in figures 6,7,8 for the different values of angle θ. From these figures, a satisfactory agreement between experimental data and theoretical calculations is obtained, revealing this way that the proposed analysis is adequate to describe the nonlinear , strain rate dependent behavior of anisotropic materials.

6. CONCLUSIONS

The tensile behavior of epoxy-glass fiber composites at various strain rates and various angles in respect to fiber axis was formulated with a theoretical model, based on three main assumptions:

A flow rule, derived for anisotropic materials elsewhere, was modified with reference to the dyadic of a set of vectors $\mathbf{a_i}$, parallel to the material axes.

The multiplicative decomposition of the deformation gradient tensor was also taken into account. Moreover, a micromechanical model that defines the rate of plastic deformation was applied. The formulation of the strain rate effect was made by extending the concept of the scaling rules of viscoelasticity in the expression of the rate of plastic deformation. The theoretical results were in a satisfactory agreement with the experimental results of the off-axis specimens.

References

1. **Hahn Hong, T. and Tsai, S.W.** "Nonlinear Elastic Behavior of Unidirectional Composite Laminae", *J.Composite Materials,* **7**,(1973),102-118 .
2. **Green,A.E. and Adkins,J.E.**, "*Large Elastic Deformations and Nonlinear Continuum Mechanics"* Oxford Univ. Press, London,(1960)
3. **Sun, C.T. and Chen, J.L.** "A Simple Flow Rule for Characterizing Nonlinear Behavior of Fiber Composites", *J.Composite Materials,* **23,** (1989), 1009-1020.
4. **Kenaga, D., Doyle, J.F. and Sun,C.T.**), "The Characterization of Boron/Aluminum Composite in the Nonlinear Range as an Orthotropic Elastic –Plastic Material", *J.Compos.Mater.,* **21**, (1987),516-531.
5. **Weeks C.A. and Sun,C.T.** , "Modeling Nonlinear Rate-Dependent Behavior in Fiber-Reinforced Composites", *Compos.Sci.Technol.,* **58**, (1998),603-611.
6. **Thiruppukuzhi, S.V. and Sun C.T**. , "Models For the Strain-Rate Dependent Behavior of Polymer Composites", *Composites Science and Technology,* **61,** .(2001), 1-12.
7. **Tanoglu, M., McKnight, S.H., Palmese J.R. and J.W. Gilespie, J.W. JR.**, "Dynamic Stress/Strain Response of the Interphase in Polymer Matrix Composites", *Polymer Composites*, **22**/5,(2001), 621-635.
8. **Lee E.H. and Lin, D.T.** ,"Finite-Strain Elastic –plastic Theory Particularly for Plane Wave Analysis", *J.Appl. Phys.* ,**38**, (1967),19.
9. **Spathis, G. and Kontou,E.** , "An Experimental and Analytical Study of the Large Strain Response of Glassy Polymers with a Non-Contact Laserextensometer", *J.Appl. Pol.Sci.,* **71**,(1999), 2007.
10. **Spathis, G. and Kontou, E.** ,"Nonlinear Viscoelastic and Viscoplastic Response of Glassy Polymers", *Pol.Eng.Sci.,* **41**/8 ,(2001), 1337 .
11. **Khan, A.S. and Huang,S.**, "*Continuum Theory of Plasticity"*, John Wiley and Sons, Inc. New York. (1995)
12. **Rubin, M.B.**, "Plasticity Theory Formulated in Terms of Physically Based Microstructural Variables – Part I. Theory", *Int.J.Solids and Structures,* **31**/19, (1994),2635-2652.
13. **Boyce, M.C., Parks,D.M and Argon, A.S.** "Plastic Flow in Oriented Glassy Polymers",*Int.J.of Plasticity,* **5**, (1989) ,593-616.
14. **Matsuoka, S.**, "*Relaxation Phenomena in Polymers",*Hanser Publishers , Munich , (1992)
15. **Spathis,G. and Kontou, E**., "Experimental and Theoretical Description of the Plastic Behavior of Semicrystalline Polymers", *Polymer,* **39**/1 ,1998,135-142.
16. **Wolfram, S.**,"*Mathematica, A system for Doing Mathematics by Computer",*2nd ed., Wolfram Research Inc. , (1993)

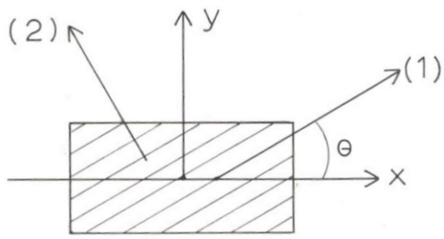

(1a)

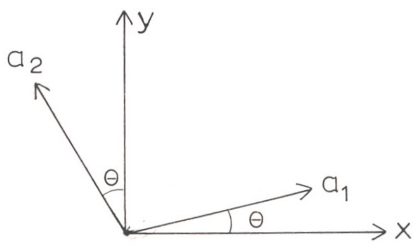

(1b)

Fig. 1 : (a) Schematic presentation of material axes and the direction of tension (x) , and (b) Schematic presentation of the relative position of vectors a_i and direction of tension (x)

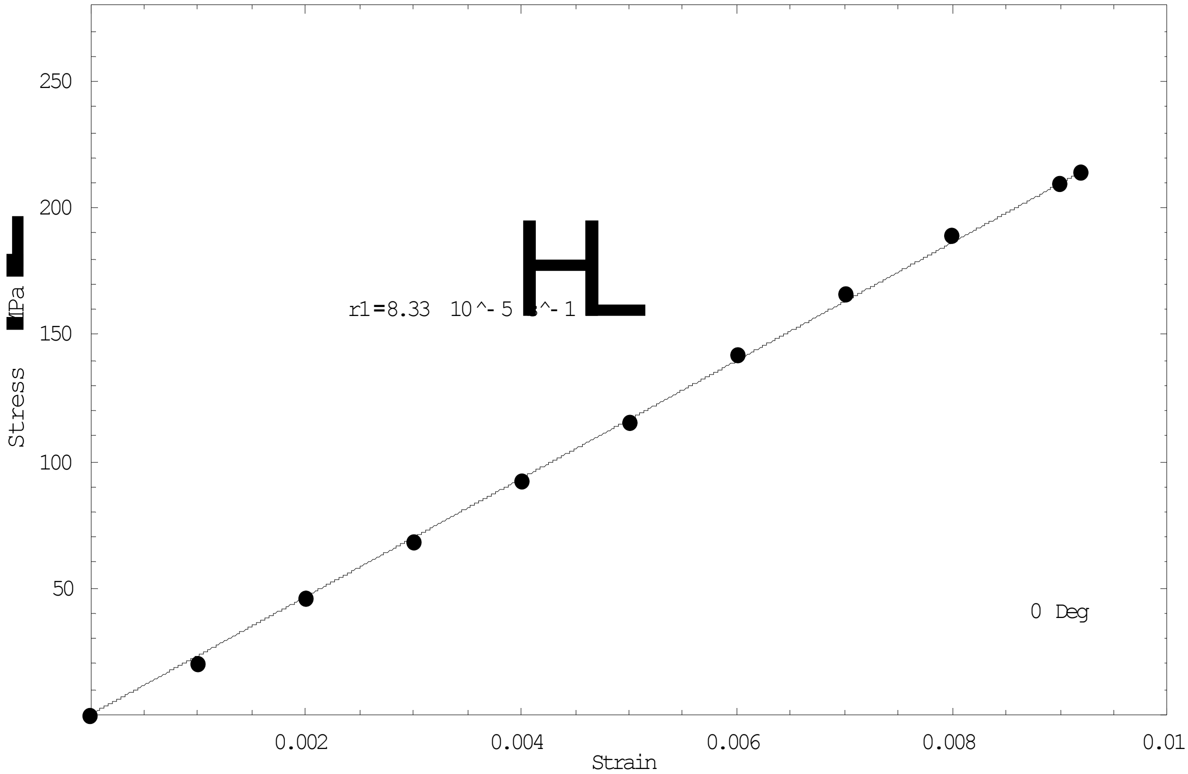

Fig. 2 : Tensile stress-strain results for $\theta=0^0$ specimen at the strain rate of 8.33 10^-5 sec^{-1} . Points: experimental results. Lines: calculated prediction in terms of elastic solution .

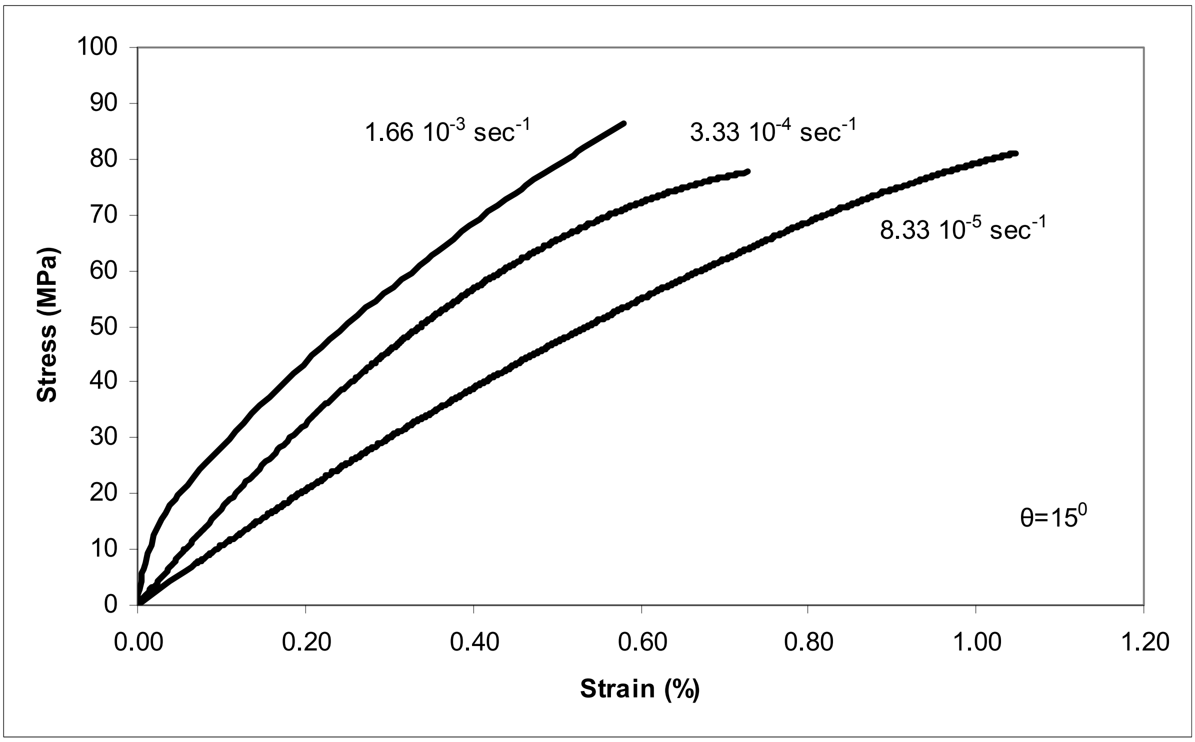

Fig. 3: Experimental tensile stress-strain curves for off-axis specimens $[15^0]$ at three strain rates.

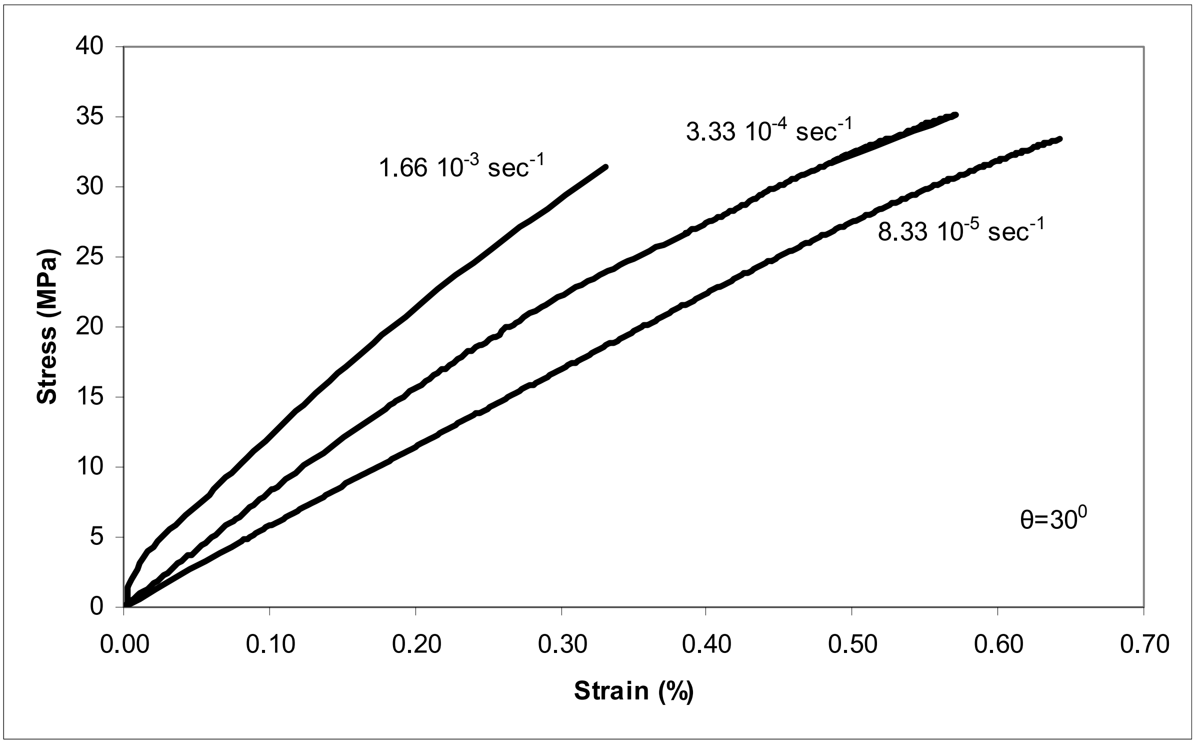

Fig. 4: Experimental tensile stress-strain curves for off-axis specimens [30^0] at three strain rates.

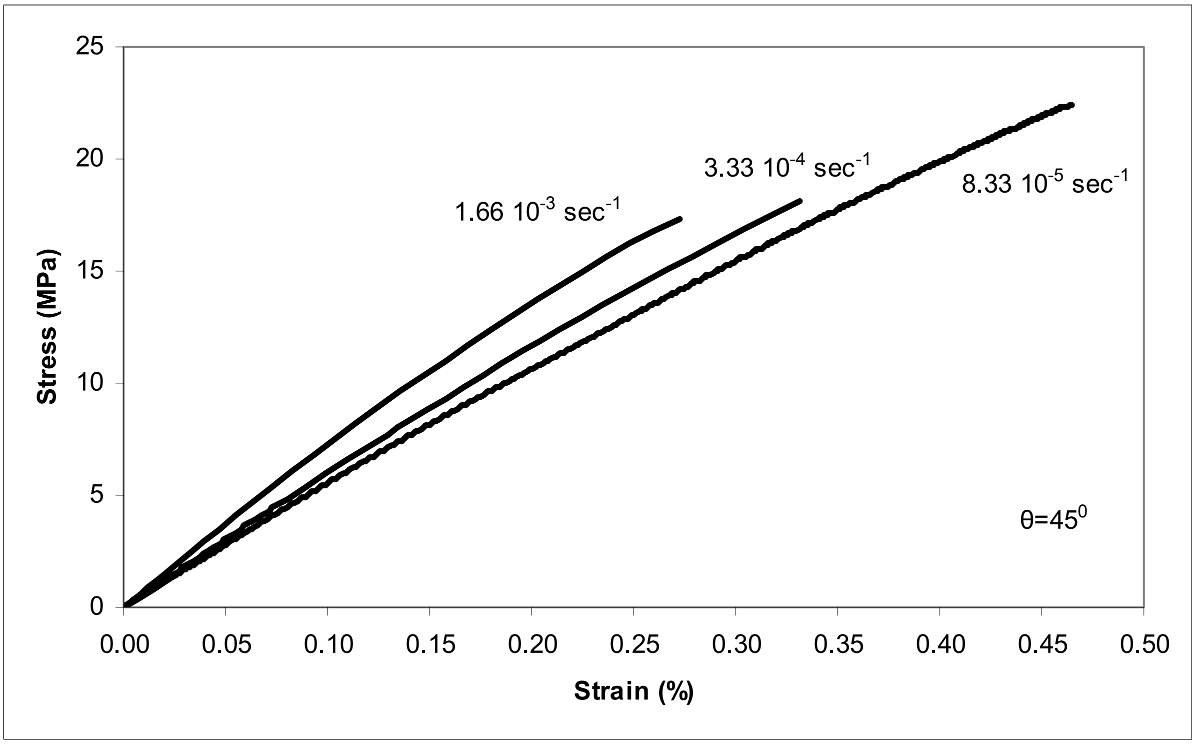

Fig. 5: Experimental tensile stress-strain curves for off-axis specimens [45^0] at three strain rates.

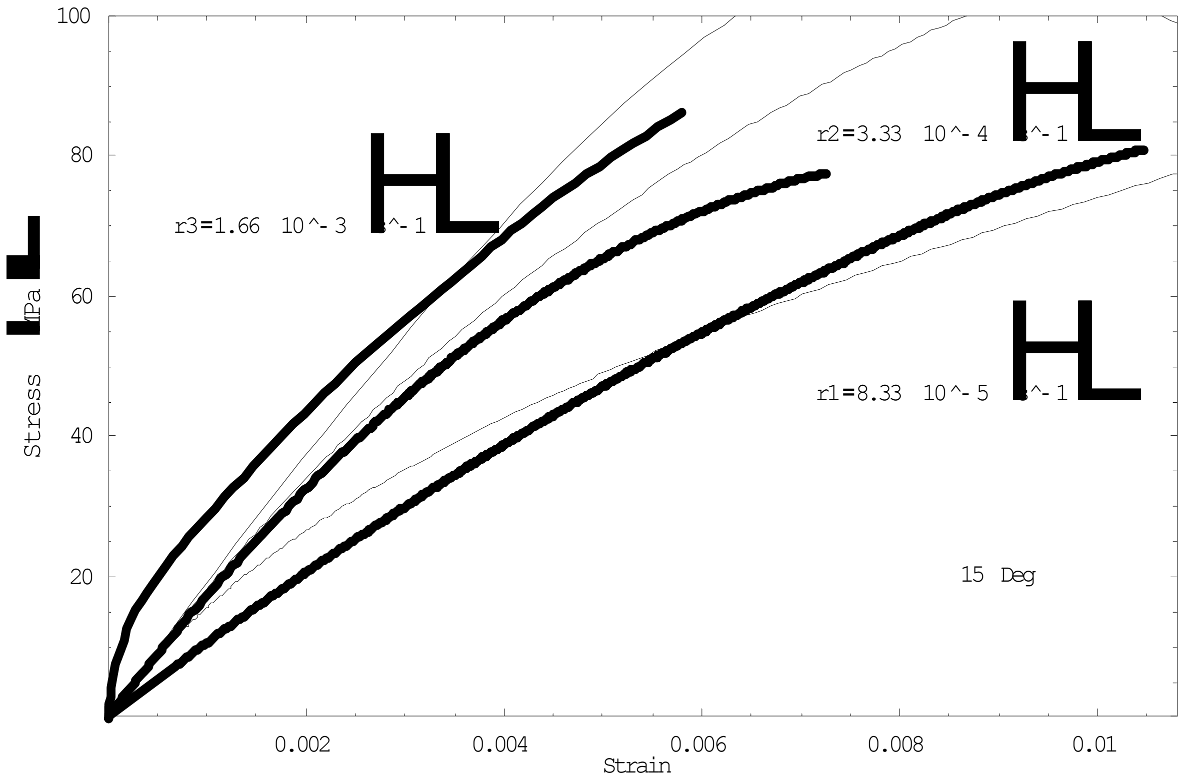

Fig. 6: Tensile stress-strain curves for $[15^0]$ at three strain rates. Bold lines: experimental data. Thin lines: calculated results

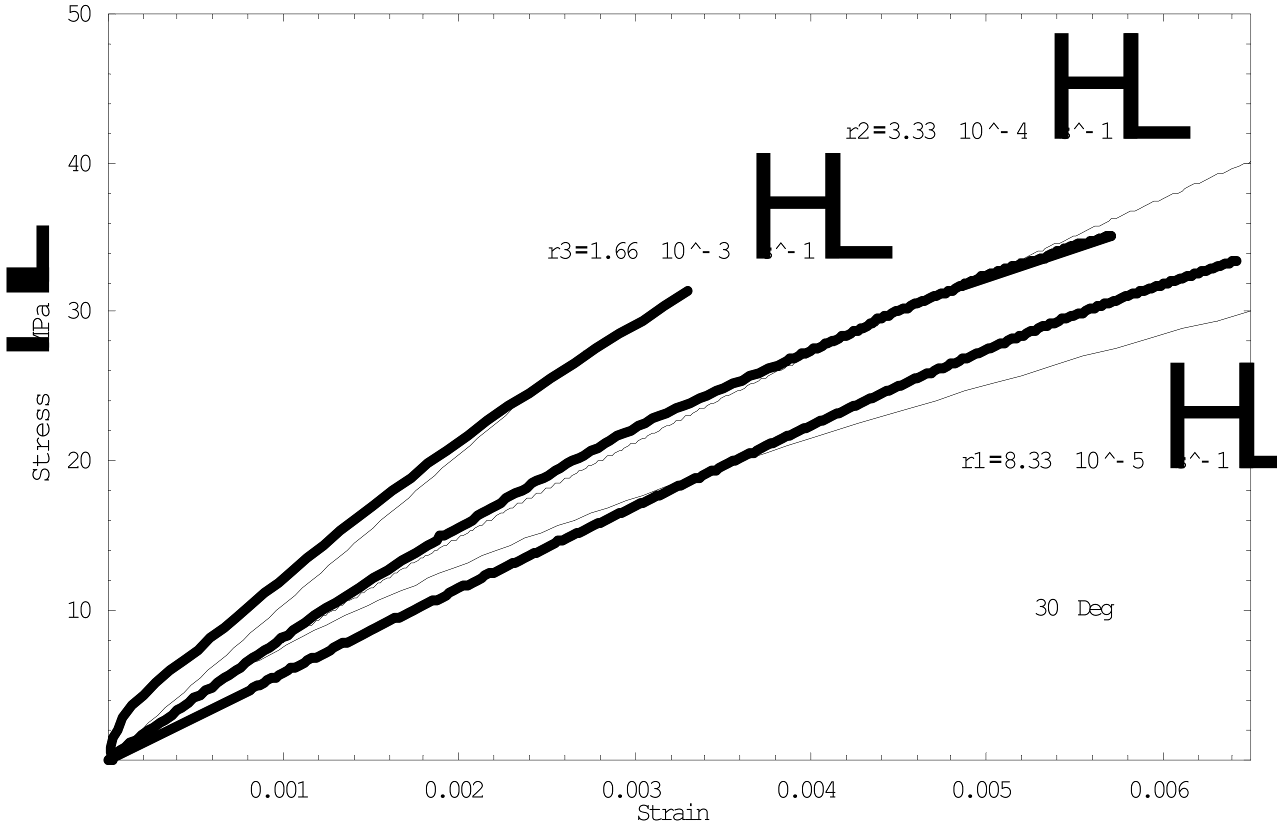

Fig. 7: Tensile stress-strain curves for $[30^0]$ at three strain rates. Bold lines: experimental data. Thin lines: calculated results

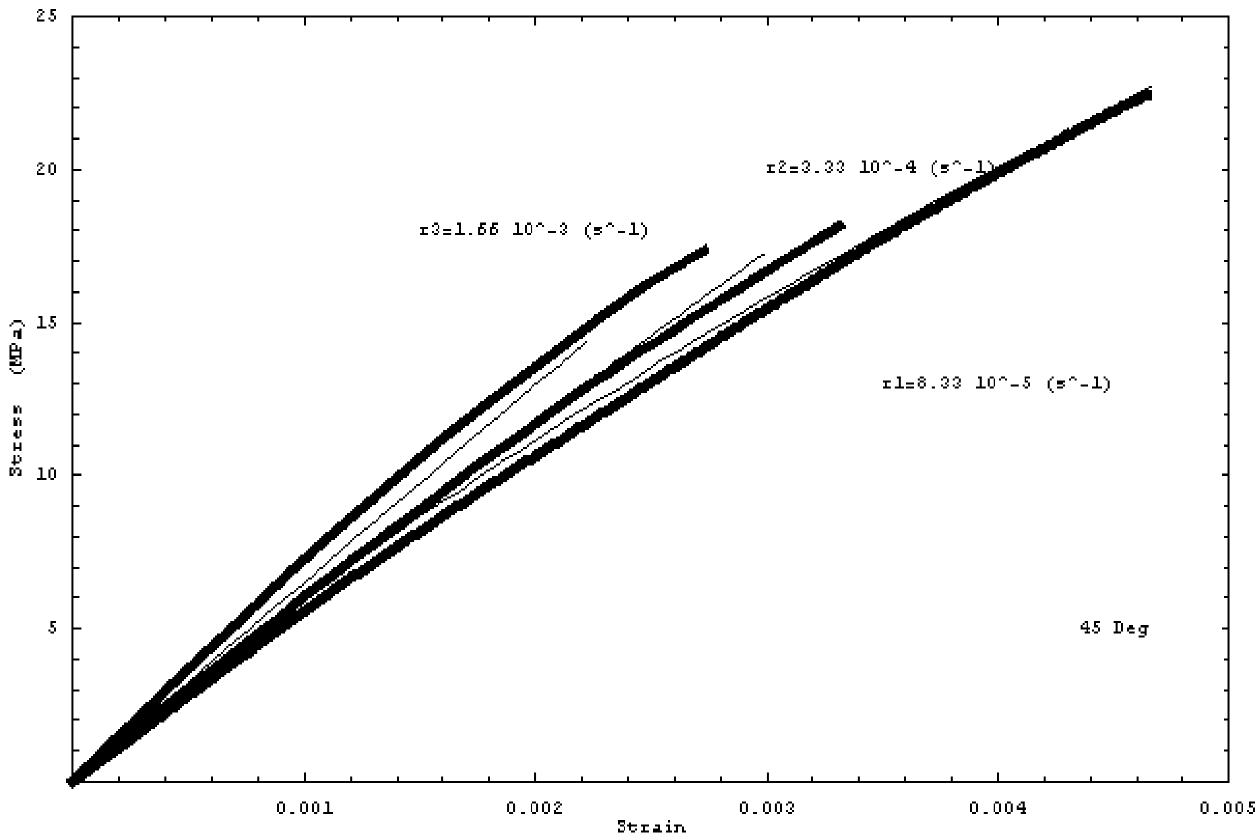

Fig. 8: Tensile stress-strain curves for [45^0] at three strain rates. Bold lines: experimental data. Thin lines: calculated results